frontiers | Frontiers in Environmental Science

ORIGINAL RESEARCH
published: 13 June 2022
doi: 10.3389/fenvs.2022.891092

Pollution Characteristics, Sources, and Health Risk Assessment of Heavy Metals in the Surface Soil of Lushan Scenic Area, Jiangxi Province, China

Shunjie Zhang[1], Hui Ye[1], Aijuan Zhang[1], Yanyu Ma[1], Qing Liu[1], Qiang Shu[1,2,3]* and Xilin Cao[3]

[1]School of Marine Science and Engineering, Nanjing Normal University, Nanjing, China, [2]Jiangsu Center for Collaborative Innovation in Geographical Information Resource Development and Application, Nanjing, China, [3]School of Geography, Nanjing Normal University, Nanjing, China

Heavy metal pollution at tourist attractions centers has caused widespread concern. In this study, the concentration of seven heavy metals (Pb, Cu, Cr, Zn, Ni, As, and Mn) in the surface soil of the Lushan scenic area was measured, and their pollution characteristics were assessed using the Nemerow comprehensive pollution index and geo-accumulation index; further, the human non-carcinogenic and carcinogenic risks were evaluated by the U.S. Environmental Protection Agency health risk assessment model. Correlation analysis, cluster analysis, and a positive matrix factorisation model were used to analyse the heavy metal sources. The results indicated that the heavy metal concentrations did not exceed the pollution threshold levels. The hazard quotients for the six heavy metals (Pb, Cu, Cr, Zn, Ni, and As) are below the threshold for non-carcinogenic health risk, whereas the carcinogenic health risk in the region is at an "acceptable" level; however, because of the high contribution of As, the carcinogenic health risks to residents of this area require continuous monitoring. Analysis revealed six sources of the pollutants: soil parent material, altitude, surface accumulation of organic matter, industrial dustfall, local human activities (life and agriculture), and tourism. These findings provide a scientific basis for developing appropriate strategies for a sustainable development of the scenic area.

Keywords: heavy metals, pollution characteristics, health risk assessment, source analysis, tourist attraction, surface soil

OPEN ACCESS

Edited by:
Juying Li,
Shenzhen University, China

Reviewed by:
Xufeng Cui,
Zhongnan University of Economics and Law, China
Adeniyi JohnPaul Adewumi,
Achievers University, Nigeria

***Correspondence:**
Qiang Shu
shuqiang@njnu.edu
xjshuqiang@sina.com

Specialty section:
This article was submitted to Soil Processes, a section of the journal Frontiers in Environmental Science

Received: *10 March 2022*
Accepted: *11 May 2022*
Published: *13 June 2022*

Citation:
Zhang S, Ye H, Zhang A, Ma Y, Liu Q, Shu Q and Cao X (2022) Pollution Characteristics, Sources, and Health Risk Assessment of Heavy Metals in the Surface Soil of Lushan Scenic Area, Jiangxi Province, China. Front. Environ. Sci. 10:891092. doi: 10.3389/fenvs.2022.891092

1 INTRODUCTION

With rapid industrialisation and urbanisation in the modern society, the increasing soil pollution has become a serious concern. Soil heavy metals are receiving increasing attention as the main soil pollutants and critical components of typical human social impacts (Huang et al., 2019). Under natural conditions, the major sources of heavy metals in the soil are biomass residues and the host rock that forms the soil (Abdu et al., 2017). The soil does have the potential to self-purify heavy metals and other pollutants (Dashko and Shidlovskaya, 2016). However, large quantities of solid wastes, such as electronic products and plastics produced by human activities, have negatively impacted the soil's ecological environment (Bongoua-Devisme et al., 2018). Furthermore, with the rapid development of the tourism industry, many tourists and construction workers enter scenic spots, inevitably generating domestic garbage, construction waste, and other wastes that add considerable manufactured heavy metal pollution to the scenic spot (Ciarkowska 2018; Brtnický et al., 2020). Heavy metal pollution is characterised by long-term concealment, easy accumulation, difficulty in degradation, irreversibility, and high toxicity. It poisons the ecological environment, affects the growth of plants and animals, and enters the human body through food chain enrichment, seriously threatening human life and health (Ali et al., 2019). The travel behaviour of tourists' affects the soil heavy metal content of the tourist destinations; further, there is a risk of accidental ingestion of polluted soils because the scenic spots are perceived to be natural and clean. Therefore, measuring the heavy metal content of surface soil in tourist attractions, evaluating its pollution characteristics, and assessing potential health risks are of great significance to the sustainable development of environmental resources in tourist destinations. In most recent studies on scenic spots, the focus has tended to be on air pollution or water pollution, and these studies confirm the need for soil pollution research. For example, Lushan Mountain's surface water has been heavily polluted because of tourism activities (Xie et al., 2020). Textile industry wastewater has polluted coastal scenic areas through watersheds (Sun et al., 2020). Through regional transport, short-duration high-intensity human tourism activities have resulted in air pollution at the scenic spots (Du et al., 2021).

Several methods for assessing soil heavy metal pollution have been developed (Chonokhuu et al., 2019; Ahn et al., 2020; Xiang et al., 2021). The Nemerow comprehensive pollution index method examines the impact of multiple contaminants in the soil and compares the study area as a whole with other areas or historical measurements. This method is widely used for soil and water pollution assessment (Wei et al., 2019) since it provides an objective evaluation based on certain regulations. The geo-accumulation index method considers the background value of each element in the soil and the influence of diagenesis on the background value, and it is a common indicator of heavy metal enrichment in the soil (Muller 1969). The U.S. Environmental Protection Agency (USEPA) health risk assessment model is widely used to quantify the carcinogenic and non-carcinogenic risks of heavy metals to humans based on the number of pollutants that enter the human body as well as their toxicity and carcinogenicity (Tepanosyan et al., 2017). This method is applicable to almost all conditions of exposure of humans to toxic substances (Arshad et al., 2020; Bayati et al., 2021). There have been health risk studies for heavy metals in beach sediments of Red Sea and Gulf of Aqaba and confirmed the safety for tourists (Nour et al., 2022). To obtain multidimensional data, this study assesses the soil pollution characteristics and health risks of the Lushan scenic area with the above three methods. Lushan is one of China's first national-level scenic spots, a world cultural heritage, and one of the nation's top 10 famous mountains, thus, an important tourism spot. Statistically, the local population of Lushan Mountain was 277,555 in 2018, and received 61,801,700 tourists, with a total tourism revenue of 40.017 billion yuan. The question arises as to whether the large number of residents, the staff serving tourists, the large number of tourists, and the large number of vehicles moving between various scenic spots in the Lushan scenic area have a significant impact on pollution at the tourist destinations as well as on the health of the residents and tourists of these scenic areas. Currently, these aspects are not clearly understood. This study aims to evaluate the pollution characteristics and health risks of heavy metal pollution in the Lushan scenic area by sampling the surface soils of tourist residences and various scenic spots in the area and analysing the sources of heavy metals to provide a scientific basis for the sustainable development of the area.

2 STUDY AREA

Lushan (29°26–29°41N, 115°52–116°08E) is a typical horst block mountain with an elliptical range located in the north of Jiangxi Province. Its north–south length is 29 km, its east–west width is approximately 16 km, and the mountain area is approximately 300 km^2. The rocks exposed in the study area are mainly feldspathic quartz sandstone, quartz sandstone and gravel-bearing quartz sandstone. Lushan Mountain is at the northern edge of China's mid-subtropical zone, which has a humid subtropical monsoon climate and at high altitude it has a distinct monsoon and mountain climate. The climate varies with altitude from subtropical to warm temperate to temperate (Feng et al., 2019). Lushan Mountain's multi-year average temperature is 11.9°C, and the annual average precipitation is 2,024 mm, which is 500 mm more than that during April to July months, the annual average relative humidity is 78%, and the annual average sunshine hours are 1,675.2 h, the frost-free period is 260 d, the annual average foggy days are up to 197.5 d, and the atmosphere is cloudy throughout the year (Feng et al., 2019). There are more than 3,000 types of plants on Lushan Mountain, which has a subtropical and subalpine landscape with a forest coverage rate of 67%, and the vegetation is a deciduous broad-leaved forest and coniferous and broad-leaved mixed forest. Conversely, 100 m below Lushan Mountain is subtropical, and the vegetation is evergreen broad-leaved forest. Due to the vertical climate variation, the distribution of organisms and soil also varies; for example, from bottom to top, the soil types are: red soil, mountain red soil, mountain yellow-red soil, mountain yellow soil, and mountain yellow-brown soil (Hu 2007).

3 MATERIALS AND METHODS

3.1 Sample Collection and Chemical Analysis

In August 2018, 49 surface soil samples were collected in Guling Town, in the Lushan scenic area along the main tourist routes where tourists and residents gather. The distribution of the sampling points is shown in **Figure 1**.

After collection, all the samples were brought to the laboratory, dried in a constant temperature drying oven at 40°C, and the plant rhizomes and other sundries were removed, and approximately 10 g of each sample was ground in an agate mortar and then manually filtered through a 200-mesh sieve. Approximately 5 g of the ground sample was weighed for preparing tablets for analysis (Shu et al., 2021). The sample tablets were placed into an X-ray fluorescence spectrometer

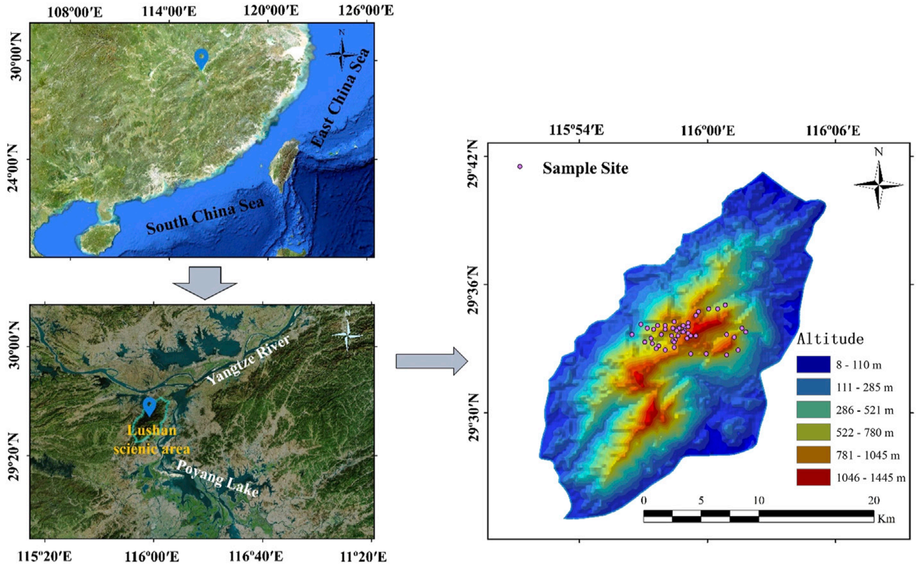

FIGURE 1 | Distribution of samples in Lushan scenic area.

(PANalytical Co., Almelo, Netherlands) for measurement; the GSS + GSD mode was selected, and the concentration of 27 elements was measured. The instrument selects Hongze Lake sediment GSS-9 (GBW07423) as the standard material for quality control, and the instrumental analysis error is less than 5%. The six heavy metals, Pb, Cu, Cr, Zn, Ni, and As, with evident biological toxicity that are also listed as priority control pollutants by USEPA, were identified. Furthermore, Pb, Cr, and As are listed as priority control metals by the Chinese government because of their high toxicity (He et al., 2013). Mn is an essential trace element in organisms, but its excessive intake can cause central nervous system damage (Sule et al., 2020). This study, therefore, primarily assessed the characteristics of heavy metal pollution and the associated health risks for the seven heavy metals Pb, Cu, Cr, Zn, Ni, As, and Mn.

3.2 Assessment of Heavy Metal Contamination

3.2.1 Pollution Characteristics

The Nemerow pollution index and geo-accumulation index were used to assess the characteristics of heavy metal pollution. Geo-accumulation index was calculated as follows:

$$I_{geo} = log_2\left(\frac{C_n}{1.5Bn}\right) \tag{1}$$

where C_n is the measured value of the heavy metal n in the sampled soil ($mg{\cdot}kg^{-1}$); B_n represents the geochemical background value of the heavy metal at the sampling site at Lushan scenic spot $mg{\cdot}kg^{-1}$; k represents the correction coefficient, considering the influence of diagenesis on the background value, k = 1.5 in this study (Kong and Zhang, 2021). The sample with I_{geo}>0, is concluded to have certain degree of contamination.

Nemerow comprehensive pollution index was calculated using **Equations 2**, **3**:

$$P_i = \frac{C_i}{S_i} \tag{2}$$

$$P_t = \sqrt{\frac{(C_i/S_i)^2_{av} + (C_i/S_i)^2_{max}}{2}} \tag{3}$$

where C_i is the actual concentration of heavy metal pollutant i in the soil ($mg{\cdot}kg^{-1}$); S_i is the evaluation standard value of the heavy metal element i in $mg{\cdot}kg^{-1}$, which refers to the *National Technical Regulations on the Evaluation of Soil Pollution Status* (MEPC, 2008) No. 39; P_i is the single pollution index of heavy metal pollutant i in the soil; (C_i/S_i)av and (C_i/S_i)max are the average and maximum values of the single pollution index of heavy metals in the soil, respectively. Generally, $P_i \leq 1$ indicates the heavy metal is non-polluting; when $1 < P_i \leq 2$, the heavy metal is in a light polluting state; when $2 < P_i \leq 3$, the heavy metal pollution is moderate (Yan et al., 2022). P_t represents the pollution index of the seven heavy metal pollutants in the surface soil of the 49 sampling locations in the Lushan scenic area. When Pt ≤ 0.7, the sampling site is in a safe state; when 0.7 < Pt ≤ 1, it means that the sampling site is in a cordon state; when 1 < Pt ≤ 2, the sampling site is in a lightly polluted state (Wang et al., 2022).

Interpolation analysis was used to estimate the above indices. The interpolation results of the Nemerow comprehensive pollution index represent the pollution status in the whole area, whereas those of the geo-accumulation index are used to analyse the spatial variations of each heavy metal element and provides a reference for source apportionment.

TABLE 1 | Values of reference dose (RfD) [mg·(kgd)$^{-1}$] and slope factor (SF) [per mg·(kgd)$^{-1}$] (Chen et al., 2016; Liu et al., 2016; Jiang et al., 2017; Zeng et al., 2019; Yu et al., 2021).

	Cr	Ni	Cu	Zn	As	Pb
RfDing	0.003	0.02	0.04	0.3	0.0003	0.0035
RfDinh	0.0000286	0.0206	0.04	0.3	0.0003	0.00352
RfDderm	0.00006	0.0054	0.012	0.06	0.000123	0.000525
SFing	—	—	—	—	1.5	0.0085
SFinh	—	0.84	—	—	15.1	—
SFderm	—	—	—	—	3.66	—

3.2.2 Health Risk Assessment

The health risk assessment of heavy metals in soil is widely used to quantify the carcinogenic and non-carcinogenic risks to humans during exposure. The basic equations for human exposure and health risk assessment (including the carcinogenic and non-carcinogenic risks of heavy metals) applied in this study are based on the recommendations and methodology for risk assessment introduced by the USEPA, including hazard identification, dose-response assessment, exposure assessment, and risk characterisation.

Step 1—Hazard identification: The aim is to determine whether exposure to these elements at the scenic spot can cause harm to human health and the probability of harm. Six heavy metals with chronic non-carcinogenic risks selected in this study included: Cr, Ni, Cu, Zn, As, and Pb. Concurrently, some heavy metals have carcinogenic risks. Therefore, these six heavy metals can harm human health after they accumulate in the human body beyond a certain limit, and the impact of these pollutants on human health is often irreversible (Huang et al., 2007).

Step 2—Dose-response assessment: This primarily includes integrating the toxicity data of Cr, Ni, Cu, Zn, As, and Pb and their carcinogenic slope. The reference coefficients used in this study are primarily derived from the carcinogenic slope factor (SF) and reference dose (RfD) of pollutants published by the USEPA. In addition, the parameters from other health risk studies were referred. The specific values are presented in **Table 1**.

Step 3—Exposure assessment: This determines the potential sensitive population in the Lushan scenic area as adults, and three exposure pathways were assumed: direct hand-mouth ingestion, respiratory system inhalation, and skin contact exposure (EPA 1989b; Ferreira-Baptista and De Miguel, 2005). The Formula for the assessment is based on the exposure parameter values such as the average weight and exposure time of the exposed population. The equations for the three exposure pathways are as follows:

$$ADD_{ing} = \mathrm{C} \times \frac{IngR \times \mathrm{CF} \times \mathrm{EF} \times \mathrm{ED}}{BW \times \mathrm{AT}} \tag{4}$$

$$ADD_{inh} = \mathrm{C} \times \frac{InhR \times \mathrm{EF} \times \mathrm{ED}}{PEF \times \mathrm{BW} \times \mathrm{AT}} \tag{5}$$

$$ADD_{derm} = \mathrm{C} \times \frac{SA \times \mathrm{CF} \times \mathrm{SSAR} \times \mathrm{ABS} \times \mathrm{EF} \times \mathrm{ED}}{BW \times \mathrm{AT}} \tag{6}$$

where $\mathrm{ADD_{ing}}$, $\mathrm{ADD_{inh}}$, and $\mathrm{ADD_{derm}}$, indicate the daily average exposure mg·(kgd)$^{-1}$ of the human body exposed to the Lushan scenic area via ingestion, inhalation, and skin contact routes, respectively. The specific meanings and values of the related parameters are listed in **Table 2**.

Step 4—Risk characterisation: Since tourism is the major business in the area, tourists were considered as objects for risk characterisation. This step calculates the potential health risks caused by the six heavy metal pollutants in the soil of the study area to tourists visiting the area by integrating the access results of the first three steps. Hazard quotient (HQ) and hazard index (HI) quantify non-carcinogenic health risks. The non-carcinogenic health risks are calculated using the following equations:

$$\mathrm{HQ}_{ij} = ADD_{ij} \big/ RfD \tag{7}$$

$$\mathrm{HQ}_i = \sum\nolimits_{j=1}^{n} HQ_{ij} \tag{8}$$

$$\mathrm{HI} = \sum\nolimits_{i=1}^{n} HQ_i \tag{9}$$

where HQ_{ij} represents the non-carcinogenic health risk of a certain heavy metal i through a single route j to the body of tourists exposed to the study area; HQ_i is the total non-carcinogenic health risk probability of a certain heavy metal i through the three exposure pathways assumed in this study to the tourists exposed to the Lushan scenic area (Chen et al., 2017); HI represents the total non-carcinogenic health risk probability of the six heavy metal pollutants through the three routes assumed in this study for the tourists exposed to the Lushan scenic area. When HQ_i or HI < 1, indicates that the non-carcinogenic health risk can be ignored; when either of these is > 1, it implies a non-carcinogenic health risk (EPA 1989a).

Carcinogenic health risk equations:

$$\mathrm{CR}_i = \mathrm{ADD}_i \times \mathrm{SF} \tag{10}$$

$$\mathrm{TCR} = \sum\nolimits_{i=1}^{n} \mathrm{CR}_i \tag{11}$$

where SF represents the slope factor of a certain heavy metal pollutant in the bodies of tourists exposed, CR_i represents the probability of cancer patients in a certain number of tourists, and TCR is the total carcinogenic risk to tourists exposed to the Lushan scenic area. According to the *Technical Guidelines for Risk Assessment of Contaminated Sites* published by the Chinese government, generally, when TCR or $\mathrm{CR}_i<10^{-6}$, it indicates no carcinogenic risk to tourists exposed to the Lushan scenic area; when 10^{-6} <TCR or $\mathrm{CR}_i<10^{-4}$, it indicates acceptable carcinogenic risk for tourists exposed to the Lushan scenic area. Pollutants within the acceptable carcinogenic risk range do not cause any harmful or undesirable health hazards to the exposed humans (EPA 1989b). Among the six heavy metal pollutants investigated in this study, Cr, Ni, As, and Pb have carcinogenic risks. Due to the lack of carcinogenic SF data for Ni and Pb exposure pathways, this study assessed the carcinogenic risk of Ni inhalation and Pb ingestion routes only. It must be noted that the carcinogenicity of Cr in the human body is due to the reduction of Cr^{6+} and production of the highly reactive intermediates Cr^{4+} and Cr^{5+} (Dayan and Paine, 2001). Cr^{3+} is an essential trace element in the human body. The

TABLE 2 | Definition and the reference values of parameters for health risk assessment of heavy metals in soils (EPA 2011).

Symbols	Units	Definition	Tourist Value
ADD	$mg \cdot (kg \cdot d)^{-1}$	Average daily exposure dose	—
C	$mg \cdot kg^{-1}$	Heavy metal concentration	Measured concentration value
ED	a	Exposure duration	0.08
BW	kg	Average body weight	61.9
CF	—	Conversion factor	10^{-6}
EF	d/a	Exposure frequency	Ignore (=1)
AT	d	Average time for carcinogenic and non-carcinogenic effects	0.08
ingR	$mg \cdot d^{-1}$	Daily oral ingestion rate of soils	100
inhR	$m^3 \cdot d^{-1}$	Daily inhalation rate of soils	12.8
PEF	$m^3 \cdot kg^{-1}$	Particulate emission factor	1.36×10^9
SSAR	$mg \cdot cm^{-2}$	Adherence rate of soil on the skin	0.07
SA	cm^2	Surface area of exposed skin for tourist	4,274
ABS	—	Absorption factor	0.001 (0.03 for As)

TABLE 3 | Variations in the concentration of heavy metal elements in the surface soil samples of Lushan Mountain ($mg \cdot kg^{-1}$).

	Cr	Ni	Cu	Zn	As	Pb	Mn
Min	37.18	13.21	7.38	52.94	4.4	17.78	157.93
Mean	74.67	25.91	18.95	95.43	11.8	38.63	502.3
Median	76.6	26	18.55	91.41	10.45	37.01	526.82
Max	98.1	35.97	30.5	152.5	25	94.71	1031.7
Standard deviation	12.46	6.19	5.71	25.5	4.33	14.82	214.91
*Coefficient of variation	0.17	0.24	0.3	0.27	0.37	0.38	0.43
Lushan Mountain background value	55.4	19.1	16.4	66.7	14.7	33.40	434
National standard value	150	40	50	200	40	80	1500
*Max (I_{geo})	0.24	0.33	0.31	0.61	0.18	0.92	0.66
*Mean (I_{geo})	-0.18	-0.19	-0.45	-0.12	-0.99	-0.47	-0.53

Note: All values except (*) are in $mg \cdot kg^{-1}$.

anthropogenic source of Cr^{6+} is primarily industrial production (Liang et al., 2021) and Cr exists in this hexavalent form mostly in alkaline soil (Pradas Del Real et al., 2020) rather than the acidic mountainous soil as in Lushan Mountain (the simultaneous traceability work also confirmed the small industrial impact here). Therefore, it is believed that the carcinogenic risk of Cr in the soil of Lushan Mountain to tourists can be ignored and cannot be calculated.

3.3 Source Apportionment of Heavy Metals

Pearson correlation analysis was used to determine the correlation between heavy metals, and cluster analysis (CA) was used to predict possible sources. Data is normalized using Z-Score. In addition, the positive matrix factorisation (PMF) model was used for source analysis for better assessment of the sources and their contribution, and this method does not have unexplainable negative values in the matrix factorisation process compared with that of the PCA method (Sofowote et al., 2008).

PMF was performed using receptor models (EPA 2014):

$$x_{ij} = \sum_{k=1}^{p} g_{ik} f_{kj} + e_{ij} \qquad (12)$$

where x_{ij} is the concentration of pollutant j measured in sample i, g_{ik} is the contribution of source k to sample i, and f_{kj} is the concentration of pollutant j in source k, and e_{ij} is the residual for each sample/pollutant.

3.4 Data Processing and Spatial Analysis

Geostatistical methods are commonly used to study and characterise the spatial distribution of pollutants in soil. This method was used to describe the spatial distribution of the pollutant concentrations in this study. The data in this study were processed using SPSS, and interpolation processing was performed using empirical Bayesian kriging (EBK) method because it has better data adaptability and predictability than other interpolation methods (Krivoruchko and Gribov, 2019) (although it also requires longer computing time). EBK interpolation was completed in ArcGIS 10.5, a box plot was constructed using R, and EPAPMF 5.0, provided by USEPA, was used for source analysis.

4 RESULTS AND DISCUSSION

4.1 Metal Element Content and Pollution Characteristics

The concentration of the seven heavy metals in the soil samples from Lushan Mountain are listed in **Table 3**. The background value of heavy metals in the soil samples in the table is taken from

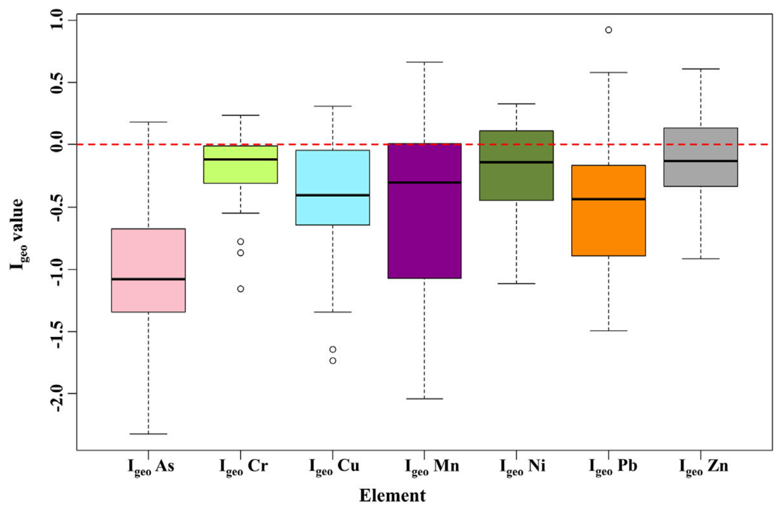

FIGURE 2 | Box plot of the relationship between the geo-accumulation index and heavy metal elements.

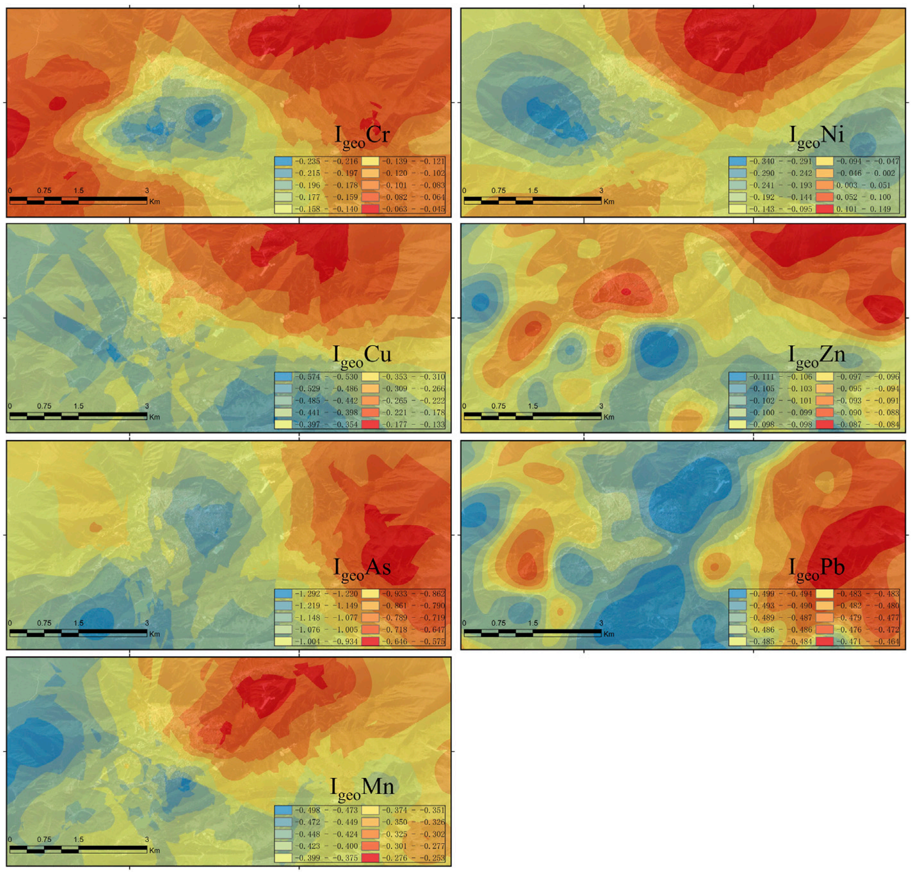

FIGURE 3 | The spatial distribution of I_{geo} values after empirical Bayesian kriging (EBK) interpolation.

the "Seventh Five-Year" National Science and Technology Research Project National Soil Environmental Background Value Research Subtopic *Soil Environmental Background Value Research in Jiangxi Province* (He et al., 2006). The national standard value is from the *National Technical Regulations on the Evaluation of Soil Pollution Status.*

TABLE 4 | Lushan scenic area soil heavy metal Nemerow comprehensive pollution index.

Site Number	Pt Value	Site Number	Pt Value	Site Number	Pt Value	Site Number	Pt Value
1	0.40	14	0.55	27	0.52	40	0.41
2	0.62	15	0.63	28	0.63	41	0.68
3	0.60	16	0.46	29	0.64	42	0.46
4	0.64	17	0.61	30	0.63	43	0.56
5	0.65	18	0.67	31	0.50	44	0.70
6	0.64	19	0.63	32	0.92	45	0.70
7	0.71	20	0.53	33	0.38	46	0.69
8	0.75	21	0.47	34	0.55	47	0.72
9	0.65	22	0.59	35	0.60	48	0.73
10	0.53	23	0.73	36	0.60	49	0.61
11	0.61	24	0.54	37	0.63	Mean	0.60
12	0.58	25	0.64	38	0.46	Max	0.92
13	0.61	26	0.46	39	0.50	—	—

TABLE 5 | Average daily exposure dose from different exposure routes in Lushan scenic area.

Element	ADDing	ADDinh	ADDderm
Cr	1.21E-04	1.14E-08	3.61E-07
Ni	4.19E-05	3.94E-09	1.25E-07
Cu	3.23E-05	3.04E-09	9.65E-08
Zn	1.54E-04	1.45E-08	4.61E-07
As	1.91E-05	1.79E-09	1.71E-06
Pb	6.24E-05	5.87E-09	1.87E-07

TABLE 6 | Non-carcinogenic health risks under different exposure routes.

Element	HQ_{ing}	HQ_{inh}	HQ_{derm}	HI
Cr	4.02E-02	3.97E-04	6.02E-03	4.66E-02
Ni	2.09E-03	1.91E-07	2.32E-05	2.12E-03
Cu	8.06E-04	7.59E-08	8.04E-06	8.15E-04
Zn	5.14E-04	4.84E-08	7.69E-06	5.22E-04
As	6.36E-02	5.98E-06	1.39E-02	7.75E-02
Pb	1.78E-02	1.67E-06	3.56E-04	1.82E-02
Sum	1.25E-01	4.05E-04	2.03E-02	1.46E-01

TABLE 7 | Carcinogenic health risks of heavy metals in Lushan scenic area.

Element	CR_{ing}	CR_{inh}	CR_{derm}	TCR
Ni	—	3.31E-09	—	3.31E-09
As	2.86E-05	2.71E-08	6.26E-06	3.49E-05
Pb	5.30E-07	—	—	5.30E-07
Sum	2.91E-05	3.04E-08	6.26E-06	3.54E-05

After calculating the pollutant concentration in the soil sample using **Formula 1**, the geo-accumulation index of the heavy metals at each sample point was obtained. **Figure 2** shows the relationship between the distribution of the geo-accumulation index and heavy metal elements in box plots.

The average and median values of the accumulation index of heavy metals in the Lushan scenic area are less than 0, indicating that the area is generally pollution-free (see **Table 3**). Among the seven elements, the average values for the accumulation index of Cr, Ni, and Zn were relatively higher, and the Q3 (upper quartile) of Ni and Zn in the box plot exceeded the pollution-free warning line (**Figure 2**). Chromium and its salts are widely used as raw materials in the chemical, electroplating, tanning, and several other industries, which are the sources of chromium-containing liquid and gaseous wastes (GracePavithra et al., 2019). Ni pollution primarily comes from industrial wastes, gas, and fuel combustion (Chaharlang et al., 2016). There are multiple sources of Zn, major being manufacturing activities such as smelting (Li et al., 2015) and traffic exhaust gases (Johansson et al., 2009).

The coefficient of variation (CV) statistically shows the degree of change in the observed values of the sample. Classical statistics classifies CV as follows: $CV \leq 0.1$ indicates weak variation, $0.1 < CV < 1$ indicates medium variation, and $CV > 1$ indicates high variation (Nielsen and Wendroth, 2003). In this study, the CV of the observed values of the concentration of each element is in the medium variation range, indicating that each element in the soil has a medium degree of spatial variation. Among these, Mn had the highest CV because Mn is primarily derived from soil-forming parent material in the soil, and it is inferred that the spatial variation of heavy metals in the study area is affected by the manufactured and natural sources.

For a better understanding of each element's spatial variation, I_{geo} values were used, and the search neighbourhoods of I_{geo}Zn and I_{geo}Pb were found to be smooth circles, whereas the others were standard circles. Compared with the concentration value, the I_{geo} value not only reflects the spatial variation of the element's concentration but also standardises the concentration of each element, which is more relevant for discovering the similarities and differences of the changes caused by human activities. As shown in **Figure 3**, some commonalities in the spatial distribution of certain elements can be found: Ni, Cu, and Mn have high-value areas in almost the same location (north of the town), and their impact has spread to the town; As and Pb have similar high-value areas to the east of the town and the second high-value area to the west of the town; the distribution of Zn is similar to that of Pb, but Zn has a high-value area in the town; Cr has two high-value areas to the north (similar to the Cu group) and west of the town which encircle the town. These commonalities imply that some of the

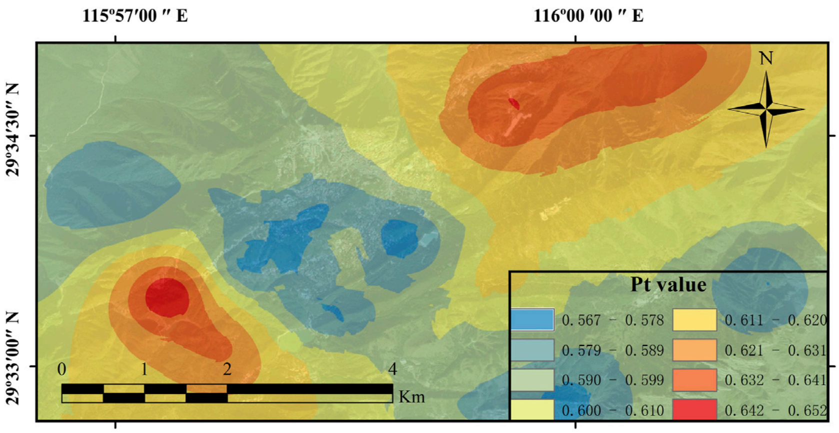

FIGURE 4 | The spatial distribution of Pt values after empirical Bayesian kriging (EBK) interpolation.

TABLE 8 | Pearson correlation coefficient of the concentration of each element.

	Cr	Mn	Ni	Cu	Zn	As	Pb	TP	Altitude
Cr	1	—	—	—	—	—	—	—	—
Mn	0.068	1	—	—	—	—	—	—	—
Ni	0.541**	0.410**	1	—	—	—	—	—	—
Cu	0.145	0.234	0.161	1	—	—	—	—	—
Zn	0.168	0.441**	−0.096	0.418**	1	—	—	—	—
As	0.345*	−0.017	−0.148	0.274	0.283*	1	—	—	—
Pb	−0.095	−0.095	−0.496**	0.508**	0.511**	0.529**	1	—	—
TP	0.085	0.151	−0.370**	0.342*	0.709**	0.276	0.586**	1	—
Altitude	−0.304*	0.161	0.03	−0.096	−0.04	−0.121	0.001	−0.049	1

*Note: *Correlation is significant at the 0.05 level. **Correlation is significant at the 0.01 level.*

pollutants have similar sources, but there is no doubt that the town is more affected by the surrounding heavy metal sources than internal sources. This phenomenon implies that in areas with complex geological environments such as the Lushan Mountain, the effect of soil parent material on heavy metals cannot be ignored (Zinn et al., 2020). This study focuses more on the phenomenon of accumulation of the heavy metal pollutants. These artificially constructed groups of elements can be used as motivations or references in subsequent studies on processes and accumulation mechanisms.

Equation 2 and **3** were used to calculate the Nemerow comprehensive pollution index (Pt) for each sample location, and the data are shown in **Table 4**. The Pt value is interpolated by the EBK method (**Figure 4**) to show a spatial change in the image map. The data transformation type is empirical, the semi-mutation model type is K_BESSEL, and the search neighbourhood is a standard circle. The layer transparency was maintained at 20%.

The highest Pt value in the study area is 0.92 (**Table 4**), which is below the pollution warning line. The highest value appeared at sample point No. 32 near Longgong Road. Notably, although the colour bar used in the interpolation layer expresses high values in red, the highest value in the interpolation result is only 0.65. After the interpolation process, the Pt value of this area is in a low and stable state (0.567–0.652), two high-value areas appear northeast and southwest of the town, and the urban area is a low-value area. The high-value areas in the northeast are primarily distributed in the tea plantations and scenic spots, and the high-value area in the southwest is centred on the famous scenic spot Datianchi in Lushan Mountain. This phenomenon shows that the heavy metal content in the region tends to be affected by tourism activities and natural factors.

4.2 Health Risk Assessment Results

4.2.1 Exposure Assessment

The major source of activity in this area is tourism, hence, this study considered the tourist group as the object to conduct health risk assessment. According to the recommended playtime in the Lushan scenic area, the duration of play was 2–3 days, the exposure duration was ED = 2.5d = 0.08a, and the exposure frequency EF was negligible. Furthermore, *Report on the Nutrition and Chronic Disease Status of Chinese Residents* shows that the average weight of the Chinese population is BW = 61.9 kg. Furthermore, it is assumed that each tourist visits the Lushan scenic area only once in his lifetime; therefore, the carcinogenic and non-carcinogenic substance exposure time AT is considered to be 0.08. **Table 5** shows the average daily exposure doses from different exposure routes in the Lushan scenic area.

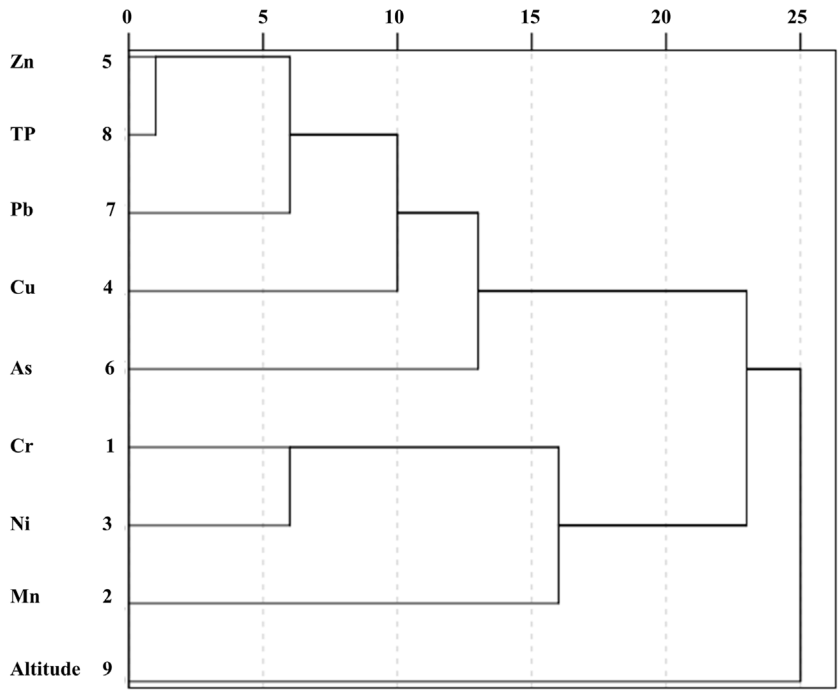

FIGURE 5 | Heavy metal cluster analysis (CA) dendrogram.

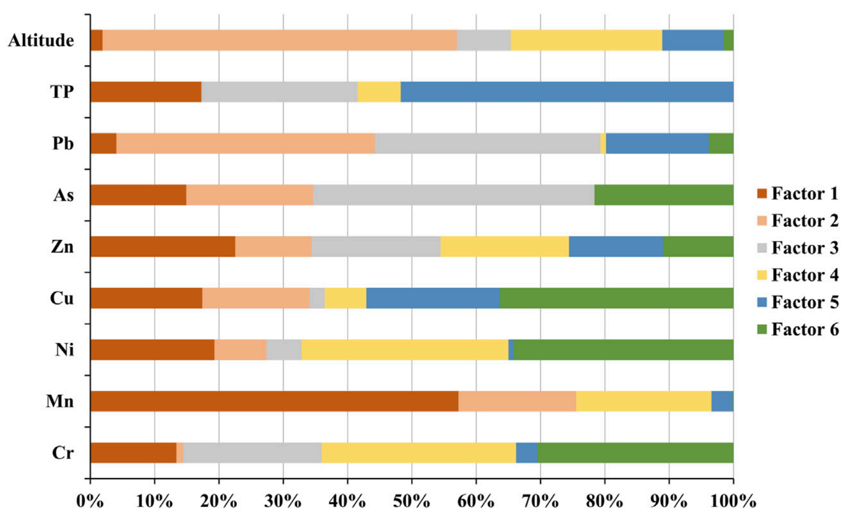

FIGURE 6 | Heavy metal factor fingerprints in Lushan scenic area.

The data in **Table 5** shows that tourists visiting Lushan scenic area are likely to be exposed to a maximum daily average pollutant dose through hand-mouth ingestion, followed by the skin contact route, and the least exposure is via inhalation. This suggests that ingestion is a significant route of human exposure to heavy metals, which is consistent with the findings of previous studies (Chonokhuu et al., 2019; Yu et al., 2021). Therefore, developing good outdoor hygiene habits: washing hands frequently and avoiding hand-mouth contact are effective ways to reduce heavy metal exposure (and also infectious diseases).

4.2.2 Non-carcinogenic Health Risks

Similar to the data for exposure assessment (**Table 5**), the non-carcinogenic health risks in the Lushan scenic area are also

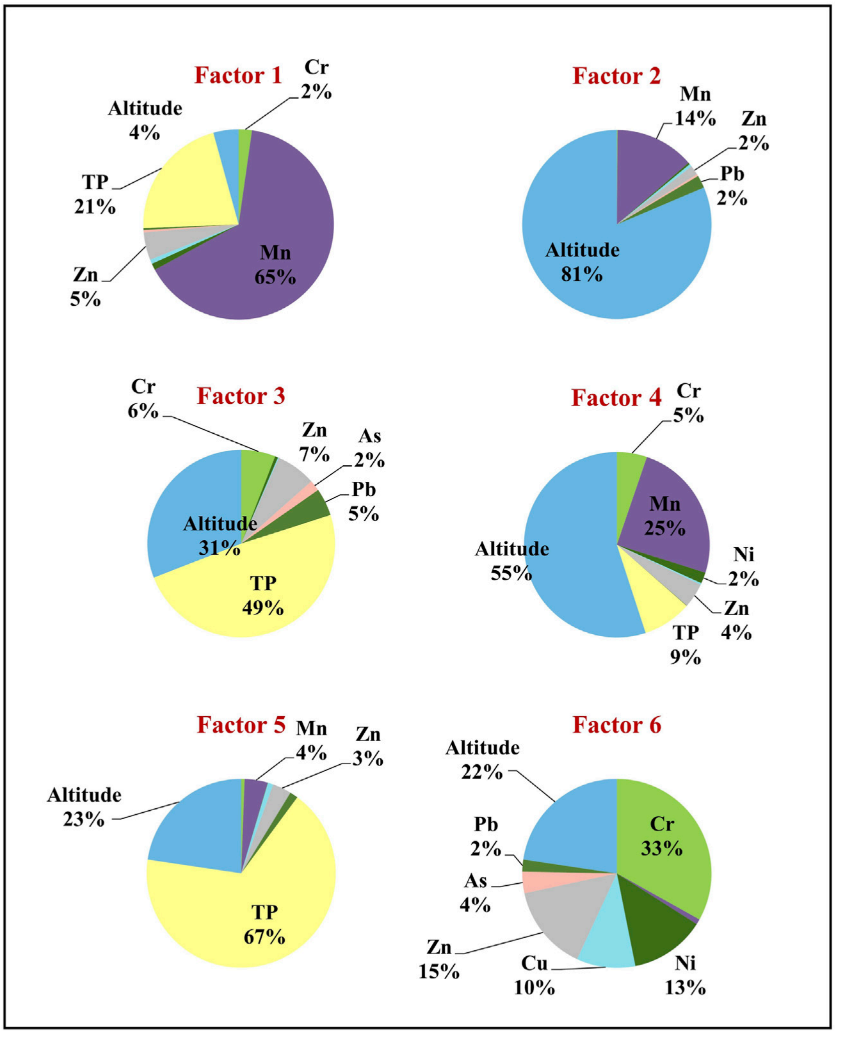

FIGURE 7 | Contribution of heavy metals (% of total factor).

dominated by hand and mouth ingestion (**Table 6**). The HQ contributed by Cr and As is higher (85% in total); however, they are still far below the safety threshold and not likely to cause any non-carcinogenic health risks to tourists exposed to the Lushan scenic area. Due to the variability of environment, it is important to take conservative estimates when assessing health risks. In the non-carcinogenic health risk assessment, the different valency states of Cr are not distinguished, and the RfD of the more toxic Cr^{6+} is uniformly used. Likewise, the RfD for inorganic form of As was used to calculate the HI for total As. Therefore, the HQ for these two heavy metals is overestimated.

4.2.3 Carcinogenic Health Risks

The carcinogenic health risks calculated using **Eq. 10** and **Eq. 11** according to the carcinogenic SF data are shown in **Table 7**.

According to the USEPA soil treatment standards, since the calculated carcinogenic health risk values for Ni and Pb are lower than 10^{-6}, their carcinogenic risk is nil, and the risk values for As are lower than 10^{-4}, which fall within the acceptable range. The highest carcinogenic health risk is from As, and oral intake is the most probable route of exposure. The TCR was lower than 10^{-4}, which is still acceptable; thus, we can conclude that in the Lushan scenic area, concentration of none of the heavy metals is high enough to cause cancer. However, the accumulation of heavy metals in the soil surface under the influence of numerous factors may pose a threat of low carcinogenic health risk in the Lushan scenic area. Hence, there is a need for continuous attention in this regard. Carcinogenesis being a long-term process, such a minimal risk may pose a threat to the residents living in towns within the scenic spot.

Although the non-carcinogenic and carcinogenic health risks in the study area are at safe levels, high HIs from Cr and As and high CRs from As indicate that Cr and As are potential health threats in the area. This trend is similar to the health risk assessment data of a rural-industrial town in Jiangsu Province from a previous study (Jiang et al., 2017). To protect the health of tourists and residents in Lushan scenic area, the anthropogenic sources of Cr and As need to be carefully monitored.

4.3 Analysis of Possible Sources of Heavy Metals

Source identification is a challenge due to lack of historical data, since most of the pollution monitoring studies have focused on plains due to the poor continuity and regularity of mountain soils. In this study, several analytical methods and reference factors were used in combination for traceability and to obtain reasonable and more realistic results. Because the concentration of total phosphorus (TP) in the soil is related to agricultural activities and natural biological processes (Katayama et al., 2021; Zhang et al., 2021), it is a better indicator for the source. Lushan Mountain has complex geomorphic conditions, and altitude is considered a potential factor affecting the spatial distribution of heavy metals (Ding et al., 2017). Therefore, in the traceability analysis, the TP and the altitude of the sample point were used as references.

The Pearson correlation coefficient used to determine the potential relationship between the concentration of heavy metals (**Table 8**), found a significant correlation between most heavy metal elements. TP was significantly positively correlated with Cu, Zn, and Pb, and significantly negatively correlated with Ni, and altitude was significantly negatively correlated with Cr. Such a complicated relationship shows that various factors are affecting the distribution of heavy metals.

In CA, the elements are divided into four categories at 15 distances (**Figure 5**): Zn, Pb, Cu, As, and TP are considered in one category; Cr and Ni are placed together; Mn and altitude are considered as one. At a distance of 20, Mn, Cr, and Ni were classified into one category. This shows that altitude has a limited impact on the distribution of heavy metals, and as an influencing factor on mountain soil and parent material. Mn is primarily affected by natural sources in the soil (Dong et al., 2019), whereas TP tends to be affected by human activity; therefore, it can be temporarily placed in a group that is more affected by human activities, such as Zn, Pb, Cu, and As, and a lower group, Cr, Ni, and Mn.

In running the PMF model, the residual error (95.2%) of most data was within ±3% when six factors were selected. Therefore, it is believed that the PMF model identified six possible sources (**Figure 6**). **Figure 7** shows the proportion of each element's contribution to this factor. Factor 1 contributes most of the Mn, which is considered to be the parent material for soil formation; Factor 2 primarily comes from the altitude and has little effect on each element, which is considered to be the effect of altitude on the concentration of heavy metals; Factor 3 primarily comes from TP, which contributes significantly to As. According to the *Soil Environmental Background Value Research in Jiangxi Province*, surface accumulation of As in the Lushan Mountain soil is evident. Other elements are more leached, whereas the surface accumulation is considered to be caused by organic matter. Factor 4 primarily comes from altitude, which exerts a certain impact on Cr, Ni, Mn, and Zn and is considered to be an industrial source (local construction and industrial dustfall); Factor 5 primarily comes from TP, which has an impact on Pb, Zn, and Cu. It is considered a local human influence (life and agriculture) in Lushan Mountain. Factor 6 has almost no effect on Mn and TP and indicates more effect on Cr, Ni, and Cu, which is considered the traffic impact caused by tourism. After removing the contribution of each element to altitude and TP, the impact on heavy metals was analysed, and the proportions of each factor was 43.24, 16.53, 7.14, 20.53, 5.59, and 6.96%, for factors 1–6, respectively, indicating that the parent material plays a major role in the heavy metal concentration, followed by industrial sources and tourism related activities.

Compared with some source apportionments of agricultural areas and mining regions (Guan et al., 2018; Motswaiso et al., 2022), this study has identified more possible sources. This infers the environmental complexity of Lushan scenic area. It also makes us think about whether the toxicity of heavy metals is passivated by the natural environment, and whether the environment is tolerating human influence in such an interaction area.

5 CONCLUSION

Heavy metal analysis results of the core area soil surface of the Lushan scenic area and various scenic spots show that the surface soil heavy metal pollution in the Lushan scenic area is generally non-polluting, and heavy metal pollution in the topsoil does not affect tourists upon exposure. Therefore, non-carcinogenic health risks are negligible. The carcinogenic health risks of all elements and their sum are within acceptable limits; however, continuous monitoring is needed (especially for the permanent residents). Six sources of heavy metals were identified in the research area, and these included soil parent material, altitude, surface accumulation of organic matter, industrial dustfall, local human activities (life and agriculture), and tourism. The soil-forming parent material determines 43.24% of the heavy metal distribution, followed by industrial sources. The research results provide a scientific basis for further improving the environmental quality of the Lushan scenic area and formulating a sustainable development policy for the scenic area. The mechanism by which these factors affect the heavy metal distribution in Lushan scenic area requires further research to implement specific pollution control measures.

DATA AVAILABILITY STATEMENT

The original contributions presented in the study are included in the article/supplementary material, further inquiries can be directed to the corresponding author.

AUTHOR CONTRIBUTIONS

Conceptualisation: QS, SZ; Methodology: SZ, YM, AZ, and HY; Formal analysis and investigation: QS, QL, YM, AZ, HY, and XC; Writing—original draft preparation: SZ; Writing—review and editing: QS; Funding acquisition: QS, XC, QL; Supervision: QS, XC.

FUNDING

This work was supported by the National Natural Science Foundation of China (No. 41671195).

REFERENCES

Abdu, N., Abdullahi, A. A., and Abdulkadir, A. (2017). Heavy Metals and Soil Microbes. *Environ. Chem. Lett.* 15 (1), 65–84. doi:10.1007/s10311-016-0587-x

Ahn, Y., Yun, H.-S., Pandi, K., Park, S., Ji, M., and Choi, J. (2020). Heavy Metal Speciation with Prediction Model for Heavy Metal Mobility and Risk Assessment in Mine-Affected Soils. *Environ. Sci. Pollut. Res.* 27, 3213–3223. doi:10.1007/s11356-019-06922-0

Ali, H., Khan, E., Ilahi, I., and Yang, Y. (2019). Environmental Chemistry and Ecotoxicology of Hazardous Heavy Metals: Environmental Persistence, Toxicity, and Bioaccumulation. *J. Chem.* 2019, 1–14. doi:10.1155/2019/6730305

Arshad, H., Mehmood, M. Z., Shah, M. H., and Abbasi, A. M. (2020). Evaluation of Heavy Metals in Cosmetic Products and Their Health Risk Assessment. *Saudi Pharm. J.* 28, 779–790. doi:10.1016/j.jsps.2020.05.006

Bayati, M., Vu, D. C., Vo, P. H., Rogers, E., Park, J., Ho, T. L., et al. (2021). Health Risk Assessment of Volatile Organic Compounds at Daycare Facilities. *Indoor Air* 31 (4), 977–988. doi:10.1111/ina.12801

Bongoua-Devisme, A., Bolou Bi, E., Kassin, K., Balland-Bolou-Bi, C., Gueable, Y., Adiaffi, B., et al. (2018). Assessment of Heavy Metal Contamination Degree of Municipal Open-Air Dumpsite on Surrounding Soils: Case of Dumpsite of Bonoua, Ivory Coast. *Int. J. Eng. Res. General Sci.* 6, 27–42.

Brtnický, M., Pecina, V., Vašinová Galiová, M., Prokeš, L., Zvěřina, O., Juřička, D., et al. (2020). The Impact of Tourism on Extremely Visited Volcanic Island: Link between Environmental Pollution and Transportation Modes. *Chemosphere* 249, 126118. doi:10.1016/j.chemosphere.2020.126118

Chaharlang, B. H., Bakhtiari, A. R., Mohammadi, J., and Farshchi, P. (2016). Geochemical Partitioning and Pollution Assessment of Ni and V as Indicator of Oil Pollution in Surface Sediments from Shadegan Wildlife Refuge, Iran. *Mar. Pollut. Bull.* 111, 247–259. doi:10.1016/j.marpolbul.2016.06.109

Chen, H., Teng, Y., Lu, S., Wang, Y., Wu, J., and Wang, J. (2016). Source Apportionment and Health Risk Assessment of Trace Metals in Surface Soils of Beijing Metropolitan, China. *Chemosphere* 144, 1002–1011. doi:10.1016/j.chemosphere.2015.09.081

Chen, X., Liu, M., Ma, J., Liu, X., Liu, D., Chen, Y., et al. (2017). Health Risk Assessment of Soil Heavy Metals in Housing Units Built on Brownfields in a City in China. *J. Soils Sediments* 17, 1741–1750. doi:10.1007/s11368-016-1625-9

Chonokhuu, S., Batbold, C., Chuluunpurev, B., Battsengel, E., Dorjsuren, B., and Byambaa, B. (2019). Contamination and Health Risk Assessment of Heavy Metals in the Soil of Major Cities in Mongolia. *Ijerph* 16, 2552. doi:10.3390/ijerph16142552

Ciarkowska, K. (2018). Assessment of Heavy Metal Pollution Risks and Enzyme Activity of Meadow Soils in Urban Area under Tourism Load: A Case Study from Zakopane (Poland). *Environ. Sci. Pollut. Res.* 25 (14), 13709–13718. doi:10.1007/s11356-018-1589-y

Dashko, R., and Shidlovskaya, A. (2016). Impact of Microbial Activity on Soil Properties. *Can. Geotech. J.* 53, 1386–1397. doi:10.1139/cgj-2015-0649

Dayan, A. D., and Paine, A. J. (2001). Mechanisms of Chromium Toxicity, Carcinogenicity and Allergenicity: Review of the Literature from 1985 to 2000. *Hum. Exp. Toxicol.* 20, 439–451. doi:10.1191/096032701682693062

Ding, Q., Cheng, G., Wang, Y., and Zhuang, D. (2017). Effects of Natural Factors on the Spatial Distribution of Heavy Metals in Soils Surrounding Mining Regions. *Sci. Total Environ.* 578, 577–585. doi:10.1016/j.scitotenv.2016.11.001

Dong, B., Zhang, R., Gan, Y., Cai, L., Freidenreich, A., Wang, K., et al. (2019). Multiple Methods for the Identification of Heavy Metal Sources in Cropland Soils from a Resource-Based Region. *Sci. Total Environ.* 651, 3127–3138. doi:10.1016/j.scitotenv.2018.10.130

Du, J., Liu, C., Wu, B., Zhang, J., Huang, Y., and Shi, K. (2021). Response of Air Quality to Short-Duration High-Strength Human Tourism Activities at a Natural Scenic Spot: A Case Study in Zhangjiajie, China. *Environ. Monit. Assess.* 193 (11), 697. doi:10.1007/s10661-021-09366-7

EPA (2014). *EPA Positive Matrix Factorization (PMF) 5.0 Fundamentals and User Guide*.

EPA (1989a). *Exposure Factors Handbook*.

EPA (2011). *Exposure Factors Handbook*. Final edn.

EPA (1989b). *Risk Assessment Guidance for Superfund. Volume I: Human Health Evaluation Manual (Part a)*, 41–44. Chapter 6.

Feng, X., Cao, X., Ju, W., and Liu, K. (2019). A Study on Community Characteristics of Forest Soil Bacteria in Lushan National Nature Reserve. *For. Resour. Manag.* 6, 101–107. (in Chinese). doi:10.13466/j.cnki.lyzygl.2019.06.018

Ferreira-Baptista, L., and De Miguel, E. (2005). Geochemistry and Risk Assessment of Street Dust in Luanda, Angola: A Tropical Urban Environment. *Atmos. Environ.* 39, 4501–4512. doi:10.1016/j.atmosenv.2005.03.026

GracePavithra, K., Jaikumar, V., Kumar, P. S., and SundarRajan, P. (2019). A Review on Cleaner Strategies for Chromium Industrial Wastewater: Present Research and Future Perspective. *J. Clean. Prod.* 228, 580–593. doi:10.1016/j.jclepro.2019.04.117

Guan, Q., Wang, F., Xu, C., Pan, N., Lin, J., Zhao, R., et al. (2018). Source Apportionment of Heavy Metals in Agricultural Soil Based on PMF: A Case Study in Hexi Corridor, Northwest China. *Chemosphere* 193, 189–197. doi:10.1016/j.chemosphere.2017.10.151

He, B., Yun, Z., Shi, J., and Jiang, G. (2013). Research Progress of Heavy Metal Pollution in China: Sources, Analytical Methods, Status, and Toxicity. *Chin. Sci. Bull.* 58, 134–140. doi:10.1007/s11434-012-5541-0

He, J., Xu, G., Zhu, H., and Peng, G. (2006). *Study on the Background Value of Soil Environment in Jiangxi Province*. Beijing: China Environmental Science Press.

Hu, H. (2007). Evaluation of the Service Value of the Forest Ecosystem in Lushan Mountain Nature Reserve. *Resour. Sci.* 29, 28–36. (in Chinese). doi:10.3321/j.issn:1007-7588.2007.05.005

Huang, S. S., Liao, Q. L., Hua, M., Wu, X. M., Bi, K. S., Yan, C. Y., et al. (2007). Survey of Heavy Metal Pollution and Assessment of Agricultural Soil in Yangzhong District, Jiangsu Province, China. *Chemosphere* 67, 2148–2155. doi:10.1016/j.chemosphere.2006.12.043

Huang, Y., Wang, L., Wang, W., Li, T., He, Z., and Yang, X. (2019). Current Status of Agricultural Soil Pollution by Heavy Metals in China: A Meta-Analysis. *Sci. Total Environ.* 651, 3034–3042. doi:10.1016/j.scitotenv.2018.10.185

Jiang, Y., Chao, S., Liu, J., Yang, Y., Chen, Y., Zhang, A., et al. (2017). Source Apportionment and Health Risk Assessment of Heavy Metals in Soil for a Township in Jiangsu Province, China. *Chemosphere* 168, 1658–1668. doi:10.1016/j.chemosphere.2016.11.088

Johansson, C., Norman, M., and Burman, L. (2009). Road Traffic Emission Factors for Heavy Metals. *Atmos. Environ.* 43, 4681–4688. doi:10.1016/j.atmosenv.2008.10.024

Katayama, S., Omori, T., and Tateno, M. (2021). Fresh Litter Acts as a Substantial Phosphorus Source of Plant Species Appearing in Primary Succession on Volcanic Ash Soil. *Sci. Rep.* 11 (1), 1–10. doi:10.1038/s41598-021-91078-6

Kong, C., and Zhang, S. (2021). Security Regional Division of Farmland Soil Heavy Metal Elements in North of the North China Plain. *Front. Environ. Sci.* 9, 639460. doi:10.3389/fenvs.2021.639460

Krivoruchko, K., and Gribov, A. (2019). Evaluation of Empirical Bayesian Kriging. *Spat. Stat.* 32, 1–27. doi:10.1016/j.spasta.2019.100368

Li, P., Lin, C., Cheng, H., Duan, X., and Lei, K. (2015). Contamination and Health Risks of Soil Heavy Metals Around a Lead/zinc Smelter in Southwestern China. *Ecotoxicol. Environ. Saf.* 113, 391–399. doi:10.1016/j.ecoenv.2014.12.025

Liang, J., Huang, X., Yan, J., Li, Y., Zhao, Z., Liu, Y., et al. (2021). A Review of the Formation of Cr (VI) via Cr (III) Oxidation in Soils and Groundwater. *Sci. Total Environ.* 774, 1–13. doi:10.1016/j.scitotenv.2021.145762

Liu, C., Lu, L., Huang, T., Huang, Y., Ding, L., and Zhao, W. (2016). The Distribution and Health Risk Assessment of Metals in Soils in the Vicinity of Industrial Sites in Dongguan, China. *Ijerph* 13, 832. doi:10.3390/ijerph13080832

MEPC (Ministry of Environment Protection of the People's Republic of China) (2008). National Technical Regulations on the Evaluation of Soil Pollution Status (Huanfa [2008] No. 39).

Motswaiso, F., Wang, J., Nakamura, K., Watanabe, N., and Komai, T. (2022). A Geochemical Approach for Source Apportionment and Environmental Impact Assessment of Heavy Metals in a Cu-Ni Mining Region, Botswana. *Environ. Earth Sci.* 81 (5), 138. doi:10.1007/s12665-021-10158-y

Muller, G. (1969). Index of Geoaccumulation in Sediments of the Rhine River. *Geojournal* 2 (108), 108–118.

Nielsen, D. R., and Wendroth, O. (2003). *Spatial and Temporal Statistics—Sampling Field Soils and Their Vegetation*. German: Reiskirchen.

Nour, H. E., Helal, S. A., and Wahab, M. A. (2022). Contamination and Health Risk Assessment of Heavy Metals in Beach Sediments of Red Sea and Gulf of Aqaba, Egypt. *Mar. Pollut. Bull.* 177, 113517. doi:10.1016/j.marpolbul.2022.113517

Pradas Del Real, A. E., Pérez-Sanz, A., García-Gonzalo, P., Castillo-Michel, H., Gismera, M. J., and Lobo, M. C. (2020). Evaluating Cr Behaviour in Two Different Polluted Soils: Mechanisms and Implications for Soil Functionality. *J. Environ. Manag.* 276, 111073. doi:10.1016/j.jenvman.2020.111073

Shu, Q., Zhao, Y., Hu, Z., Yang, P., Liu, Y., Chen, Y., et al. (2021). Multi-proxy Reconstruction of the Holocene Transition from a Transgressive to Regressive Coastal Evolution in the Northern Jiangsu Plain, East China. *Palaeogeogr. Palaeoclimatol. Palaeoecol.* 572, 110405. doi:10.1016/j.palaeo.2021.110405

Sofowote, U. M., Mccarry, B. E., and Marvin, C. H. (2008). Source Apportionment of PAH in Hamilton Harbour Suspended Sediments: Comparison of Two Factor Analysis Methods. *Environ. Sci. Technol.* 42 (16), 6007–6014. doi:10.1021/es800219z

Sule, K., Umbsaar, J., and Prenner, E. J. (2020). Mechanisms of Co, Ni, and Mn Toxicity: From Exposure and Homeostasis to Their Interactions with and Impact on Lipids and Biomembranes. *Biochimica Biophysica Acta (BBA) - Biomembr.* 1862 (8), 183250. doi:10.1016/j.bbamem.2020.183250

Sun, Q., Wang, X., and Wang, L. (2020). Ecological Impact of Watershed Water Pollution Control on Coastal Tourist Scenic Spots. *Int. J. Low-Carbon Technol.* 15 (1), 84–88. doi:10.1093/ijlct/ctz060

Tepanosyan, G., Maghakyan, N., Sahakyan, L., and Saghatelyan, A. (2017). Heavy Metals Pollution Levels and Children Health Risk Assessment of Yerevan Kindergartens Soils. *Ecotoxicol. Environ. Saf.* 142, 257–265. doi:10.1016/j.ecoenv.2017.04.013

Wang, T., Lou, Y., Jiang, S., Wang, J., Zhang, Y., and Pan, W.-P. (2022). Distribution Characteristics and Environmental Risk Assessment of Trace Elements in Desulfurization Sludge from Coal-Fired Power Plants. *Fuel* 314, 122771. doi:10.1016/j.fuel.2021.122771

Wei, L., Huang, C., Wang, Z., Wang, Z., Zhou, X., and Cao, L. (2019). Monitoring of Urban Black-Odor Water Based on Nemerow Index and Gradient Boosting Decision Tree Regression Using UAV-Borne Hyperspectral Imagery. *Remote Sens.* 11 (20), 2042. doi:10.3390/rs11202402

Xiang, M., Li, Y., Yang, J., Lei, K., Li, Y., Li, F., et al. (2021). Heavy Metal Contamination Risk Assessment and Correlation Analysis of Heavy Metal Contents in Soil and Crops. *Environ. Pollut.* 278, 1–10. doi:10.1016/j.envpol.2021.116911

Xie, D., Huang, Q., Xu, S., Zhou, Y., Zhou, G., Jia, J., et al. (2020). Assessment of Surface Water Quality in Lushan: a World Heritage Sites in China. *Environ. Sci. Pollut. Res.* 27, 18934–18948. doi:10.1007/s11356-020-08304-3

Yan, T., Zhao, W., Yu, X., Li, H., Gao, Z., Ding, M., et al. (2022). Evaluating Heavy Metal Pollution and Potential Risk of Soil Around a Coal Mining Region of Tai'an City, China. *Alexandria Eng. J.* 61, 2156–2165. doi:10.1016/j.aej.2021.08.013

Yu, G., Chen, F., Zhang, H., and Wang, Z. (2021). Pollution and Health Risk Assessment of Heavy Metals in Soils of Guizhou, China. *Ecosyst. Health Sustain.* 7, 1–12. doi:10.1080/20964129.2020.1859948

Zeng, S., Ma, J., Yang, Y., Zhang, S., Liu, G.-J., and Chen, F. (2019). Spatial Assessment of Farmland Soil Pollution and its Potential Human Health Risks in China. *Sci. Total Environ.* 687, 642–653. doi:10.1016/j.scitotenv.2019.05.291

Zhang, H., Yin, A., Yang, X., Fan, M., Shao, S., Wu, J., et al. (2021). Use of Machine-Learning and Receptor Models for Prediction and Source Apportionment of Heavy Metals in Coastal Reclaimed Soils. *Ecol. Indic.* 122, 1–11. doi:10.1016/j.ecolind.2020.107233

Zinn, Y. L., Faria, J. A., Araujo, M. A., and Skorupa, A. L. A. (2020). Soil Parent Material Is the Main Control on Heavy Metal Concentrations in Tropical Highlands of Brazil. *Catena* 185, 1–11. doi:10.1016/j.catena.2019.104319

Conflict of Interest: The authors declare that the research was conducted in the absence of any commercial or financial relationships that could be construed as a potential conflict of interest.

Publisher's Note: All claims expressed in this article are solely those of the authors and do not necessarily represent those of their affiliated organizations, or those of the publisher, the editors and the reviewers. Any product that may be evaluated in this article, or claim that may be made by its manufacturer, is not guaranteed or endorsed by the publisher.